Cardiovascular Engineering and Technology, Vol. 13, No. 6, December 2022 *(© 2022)* pp. 872–885
https://doi.org/10.1007/s13239-022-00623-5

Original Article

Effect of Cyclic Uniaxial Mechanical Strain on Endothelial Progenitor Cell Differentiation

PRASHANTH RAVISHANKAR,[1] ISHITA TANDON,[1] and KARTIK BALACHANDRAN [1,2]

[1]Department of Biomedical Engineering, University of Arkansas, 700 W Research Center Blvd, Fayetteville, AR 72701, USA; and [2]Department of Biomedical Engineering, University of Arkansas, 122 John A. White Jr. Engineering Hall, Fayetteville, AR 72701, USA

(Received 6 November 2021; accepted 30 March 2022; published online 2 May 2022)

Abstract
Purpose—Endothelial progenitor cells (EPCs) have been used as an autologous or allogeneic source in multiple tissue engineering applications. EPCs possess high proliferative and tissue regeneration potential. The effect of shear stress on EPCs has been extensively studied but the role of cyclic mechanical strain on EPCs remains to be understood. In this study, we focused on examining the role of uniaxial cyclic strain on EPCs cultured on three-dimensional (3D) anisotropic composites that mimic healthy and diseased aortic valve tissue matrix compositions.
Methods and Results—The composites were fabricated by combining centrifugal jet spun fibers with photocrosslinkable gelatin and glycosaminoglycan hydrogels. A custom-designed uniaxial cyclic stretcher was used to provide the necessary cyclic stimulation to the EPC-seeded 3D composites. The samples were cyclically strained at a rate of 1 Hz at 15% strain mimicking the physiological condition experienced by aortic valve, with static conditions serving as controls. Cell viability was high in all conditions. Immunostaining revealed reduced endothelial marker (CD31) expression with increased smooth muscle cell marker, SM22α, expression when subjected to cyclic strain. Functional analysis through Matrigel assay agreed with the immunostaining findings with reduced tubular structure formation in strained conditions compared to EPC controls. Additionally, the cells showed reduced acLDL uptake compared to controls which are in alignment with the EPCs undergoing differentiation.
Conclusion—Overall, we show that EPCs lose their endothelial progenitor phenotype, and have the potential to be differentiated into mesenchymal-like cells through cyclic mechanical stimulation.

Keywords—Endothelial progenitor cells, Anisotropic valve-mimetic fiber-reinforced hydrogel scaffolds, Uniaxial cyclic mechanical strain, Heart valve tissue engineering.

INTRODUCTION

Endothelial progenitor cells (EPCs) have gained a lot interest since their discovery in 1997 by Ashara *et al.*,[2] and have been studied both as an autologous and allogeneic source for tissue engineering and regenerative medicine applications.[15,14,1118] EPCs possess a high proliferative potential and play an important role in neovascularization by mobilizing to injury sites and remodeling the tissue.[12,24,2840] These cells are found in the bone marrow, peripheral blood, umbilical cord blood, and as tissue residents.[28,33,39] As these cells can be obtained with minimally invasive techniques, it makes them a valuable cell source for tissue regeneration.

Mechanical forces such as shear stress and stretch tension have been shown to affect the endothelial cells to change cell shape, function, and gene expression.[25,13,35] Several studies have been conducted to understand the role of shear stress in EPC differentiation to mature endothelial cells *via* the expression of endothelial cell markers like Tie2, VE-cadherin, von Willebrand factor (vWF), vascular endothelial growth factor receptors 1 and 2 (VEGFR1, VEGFR2).[25,13,34,26,6] EPCs experiencing shear stress also exhibited increased expression of adhesion molecules such as E-selectin, ICAM1, and VCAM1.[25,1] Interestingly, EPCs when treated with soluble factors like transforming growth factor β (TGFβ) or plate-

Address correspondence to Kartik Balachandran, Department of Biomedical Engineering, University of Arkansas, 700 W Research Center Blvd, Fayetteville, AR 72701, USA. Electronic mail: kbalacha@uark.edu

let-derived growth factor, have been reported to differentiate into smooth muscle cells with increased expression of α smooth muscle actin (αSMA) and transgelin (SM22α).[8,23,37,38] These observations indicate that EPCs can be used as a potential cell source that can differentiate and provide smooth muscle cell-like and endothelial functions. Although studies have focused on EPC differentiation by biochemical cues and shear stresses, research still lacks on understanding how these cells respond to cyclic mechanical strain.

Microenvironmental mechanical changes can lead to cell behavioral changes and in turn alter the tissue function.[5] Tissues like blood vessels and heart valves experience cyclic strains and it has been well established that mechanical strain plays an important role in remodeling of vascular grafts and blood vessels.[22,10,27,16,19] Our previous work also reported that valve endothelial cells can undergo TGFβ-mediated differentiation to valve interstitial cells in response to uniaxial cyclic mechanical strain.[3] These observations led us to study the effect of cyclic mechanical conditioning on EPCs and specifically, if cyclic conditioning would lead to EPC differentiation in a 3-dimensional (3D) platform. The response of cells to mechanical strains have not been extensively studied in 3D cultures and a need for these studies is essential as cells respond differently to mechanical stimuli in 2-dimensional cultures.[20,4]

We hypothesized that we can induce EPC differentiation into valve-like cells by culturing these cells on a 3D valve-mimetic composite in a valve-mimetic mechanical environment. To accomplish this, we used our previously reported fiber-reinforced glycosaminoglycan-based hydrogel composite that exhibits mechanical properties comparable to a native valve tissue,[31] and seeded these composites with EPCs. These EPC-seeded composites were subjected to *in vitro* cyclic strains using a custom-built uniaxial stretcher.

METHODS

Isolation and Expansion of Endothelial Progenitor Cells

Human umbilical cord blood units were received from the Arkansas Cord Blood Bank with prior approval from the University of Arkansas Institutional Review Board (#16-04-722). Two cord blood units from different donors were used in this study to obtain EPCs. Using our previously established protocol,[32] we carried out density gradient centrifugation with Ficoll-Paque to isolate the mononuclear cells (MNCs). These MNCs were plated on a collagen-I coated cell culture plate and supplemented with Endothelial Growth Medium (EGM; Lonza). The culture plates were monitored for endothelial cell colonies and maintained in culture till the colonies reached 2-3mm in size. These colonies were trypsinized and plated in a collagen-I treated cell culture flask supplemented with EGM for expansion. The isolated EPCs were immunostained to ensure their phenotype and based on our previous results for EPC marker expression,[32] passages 1-3 were used for the following proposed experiments.

Preparation and Attachment of Valve-Mimetic Composites to Elastomeric Membranes

Elastomeric polydimethylsiloxane (PDMS) sheets (Specialty Manufacturing Inc, Michigan) were cut to dimensions (8 by 7 cm) and spin coated with freshly prepared PDMS to attach a silicone ring that would serve as a chamber for cell culture. To enable the attachment of the valve-mimetic composites to the elastomeric sheets, the chambers were activated using plasma treatment and chemically treated with benzophenone (10% w/v in acetone) for 15 min.[42] After the treatment, the chambers were washed once with methanol, thrice with deionized water, and blow dried with nitrogen gas prior to the attachment of valve-mimetic composites.

Based on our previous publication,[31] healthy and diseased fiber-reinforced hydrogel composites were fabricated by combining centrifugal jet spun polycaprolactone (PCL):gelatin fibers and photocrosslinkable forms of gelatin and glycosaminoglycans (GAGs). The fibers were fabricated by centrifugal jet spinning a 8% w/v solution mixture of 3:1 PCL:Gelatin.[17,30] For the hydrogel component, gelatin methacrylate (GelMA) prepolymer solutions were prepared containing 5% GelMA and 0.5% photo-initiator (Irgacure 2959).[31] 2.4 mg/ml of GAG mixture of methacrylated hyaluronic acid (HAMA) (60%) and methacrylated chondroitin sulfate (CSMA) (40%) were dissolved in the GelMA prepolymer solution to simulate the healthy composition of GAGs found in the native valve.[7] For the diseased conditions, the GAG concentration was increased four-fold (9.6 mg/ml), as GAG enrichment is a dominant hallmark for early calcific aortic valve disease.[29] A detailed breakdown of the scaffold components is provided in Table 1.

The prepolymer solutions were added to benzophenone-treated chambers and centrifugal jet spun anisotropic PCL; gelatin fibers[30] were placed with its radial direction aligned to the direction of the stretch, mimicking the *in vivo* stretch direction. Upon complete soaking of the fibers, the scaffolds were crosslinked using UV light (365nm Blak-Ray B UV-crosslinker) at 2.6 mW/cm^2 for 45 seconds to construct and attach the fiber-reinforced hydrogel composites (hereafter called valve-mimetic composites) to the elastomeric PDMS

TABLE 1. Detailed composition of healthy and diseased anisotropic fiber-reinforced hydrogel composites.

	GelMA (mg/mL)	GAG Composition (mg/mL)	Irgacure 2959 (wt%)	PCL/Gelatin fibers (wt%)
Healthy Composite (HC)	50	Total GAG = 2.4 HAMA (60%) = 1.44 CSMA (40%) = 2.4	0.5	8% PCL/Gelatin (3 PCL: 1 Gelatin Ratio)
Diseased Composite (DC)	50	Total GAG = 2.4 HAMA (60%) = 5.76 CSMA (40%) = 9.6	0.5	8% PCL/Gelatin (3 PCL: 1 Gelatin Ratio)

membrane. An additional set of valve-mimetic composites were also made on a sterile Petri dish to characterize the scaffold's physiochemical and mechanical properties,[31,41] and are reported in the supplemental section.

Uniaxial Cyclic Mechanical Stretching of EPCs

To ensure the strain is being transmitted through the valve-mimetic composite, fiducial markers were placed on the fibers prior to crosslinking and mounted onto a custom-built uniaxial stretcher using clamps. Images were captured to the full extent of the stretch cycle and a custom MATLAB code was employed to measure the strains by marker tracking.

For uniaxial cyclic studies, 500,000 EPCs were seeded on the valve-mimetic composite surface and cultured statically overnight in EGM to ensure complete swelling of the composite and cell attachment. Stretched samples were cyclically strained at a rate of 1Hz for 15% strain in the radial fiber direction mimicking the physiological condition.[36] Static cultures supplemented with either EGM media or EGM with TGFβ served as controls. All studies were performed for 48 hours.

Evaluation of Cell Viability and Immunostaining

All samples were stained for cell viability at 48 hours using ThermoFisher live/dead viability kit. The samples were imaged using an Olympus FV10i Fluoview confocal microscope. The number of live and dead cells quantified across at least three image fields using ImageJ, and cell viability was calculated using the following formula: $\%ofCellViability = Numberof livecells/(TotalNumberoflive + deadcells) * 100$.[31]

For immunostaining, samples were fixed and permeabilized in 4% paraformaldehyde and 0.1% Triton X-100 for 15 min. Samples were then immunostained using primary antibodies for CD31 (endothelial marker), CD34 (hematopoietic stem cell marker), VEGFR2 (vascular endothelial marker), and SM22α (smooth muscle cell marker). Following primary stains, samples were stained with their appropriate secondary antibodies and included DAPI for staining the nuclei. All samples were imaged on an Olympus FV10i Fluoview confocal microscope.

Matrigel Vasculogenic Assay

A 96-well plate was coated with 50μl/well of Matrigel (Reduced Growth Factor Matrigel, Corning) and incubated in 37 °C for 30 min to ensure gelling. At the end of 48 hours, all sample conditions were washed three times with 1X phosphate buffered saline and treated with 0.05% trypsin to release the cells. The cells were centrifuged and counted to seed them onto the prepared Matrigel-coated plates at 20,000 cells/well. These plates were returned to the 37 °C incubator overnight and imaged for the cells' ability to form vascular tube-like structures upon all treatment conditions. Valve interstitial cells and untreated EPCs served as negative and positive controls, respectively. The images were quantified using ImageJ to identify the number of vascular tube structures per image field, the mean tube area, and the mean branching points.

Acetylated Low-Density Lipoprotein Uptake Assay

At the end of 48 hours, all samples were washed thrice with PBS, and incubated with Dil-acetylated low-density lipoprotein (Dil-ac-LDL, 5 mg/mL, Invitrogen) at 37 °C for 4 hours. Thereafter, the cells were washed twice with PBS, fixed using 4% paraformaldehyde for 10 min, and was followed by nuclei staining using DAPI in 2% PFA for 10 min. The samples were imaged using an Olympus FV10i Fluoview confocal microscope and were quantified using ImageJ to calculate the percentage of cells expressing acLDL uptake given by,

$$\%\text{ of cells uptaking acLDL} = \text{Number of cells uptaking acLDL}/(\text{Total number of cells analyzed by DAPI}) \times 100.$$

qRT-PCR

After 48 hours, samples were frozen in TRIzol (Invitrogen, Grand Island, NY) and stored at − 80 °C after flash freezing in liquid N_2. For isolating mRNA chloroform phase separation was performed followed by washing and elution as per the manufacturer's protocol (PureLink RNA Mini Kit, Life Technologies). Reverse transcription to cDNA was carried out using iScript RT supermix (Bio-Rad, Hercules, CA). SM22α gene expression was quantified relative to the housekeeping gene GAPDH using the SsoAdvanced Universal SYBR Green supermix (Bio-Rad) in a CFX96 real-time system (BIO-RAD). Primers for SM22α (fwd: 5′-CGGTCCCTGGCAATTCTGTTTAC-3′ rev: 5′-CTTGGTGAACTGTGCGTGTCTG-3′) and GAPDH (fwd: 5′-CAATGACCCCTTCATTGACC-3′ rev: 5′-TTGATTTTGGAGGGATCTCG-3′) were obtained from Thermofisher Scientific (Waltham, MA). The ΔCt values were normalized by the ΔCt value of 15% strained diseased composites to obtain the ΔΔCt. Fold change was then calculated as $2^{-\Delta\Delta Ct}$ and graphed.

Statistical Analysis

All studies were carried out with three to four experimental replicates unless otherwise stated. The experimental data was analyzed for statistical significance using one-way ANOVA followed by Tukey's *post-hoc* tests. Data is presented as mean ± standard error, with a p-value of less than 0.05 considered as statistically significant. Exact p-values are reported whenever appropriate.

RESULTS

Isolated Cells Were Confirmed to be EPCs

The outgrowth of EPC colonies from the seeded mononuclear cells on collagen coated plates was observed between day 5-7. Similar to our previous observations,[32] the cell colonies progressed their growth with an early spindle-shaped morphology and later progressed to a cobblestone morphology (Fig. 1a). The isolated EPCs were confirmed with immunostaining (Fig. 1b) as they stained positive for common EPC markers such as CD31 and CD34 with negative staining for smooth muscle cell marker, αSMA. Additionally, it can be noted from our Matrigel assay that the isolated EPCs that served as controls also showed the ability to form vascular-like

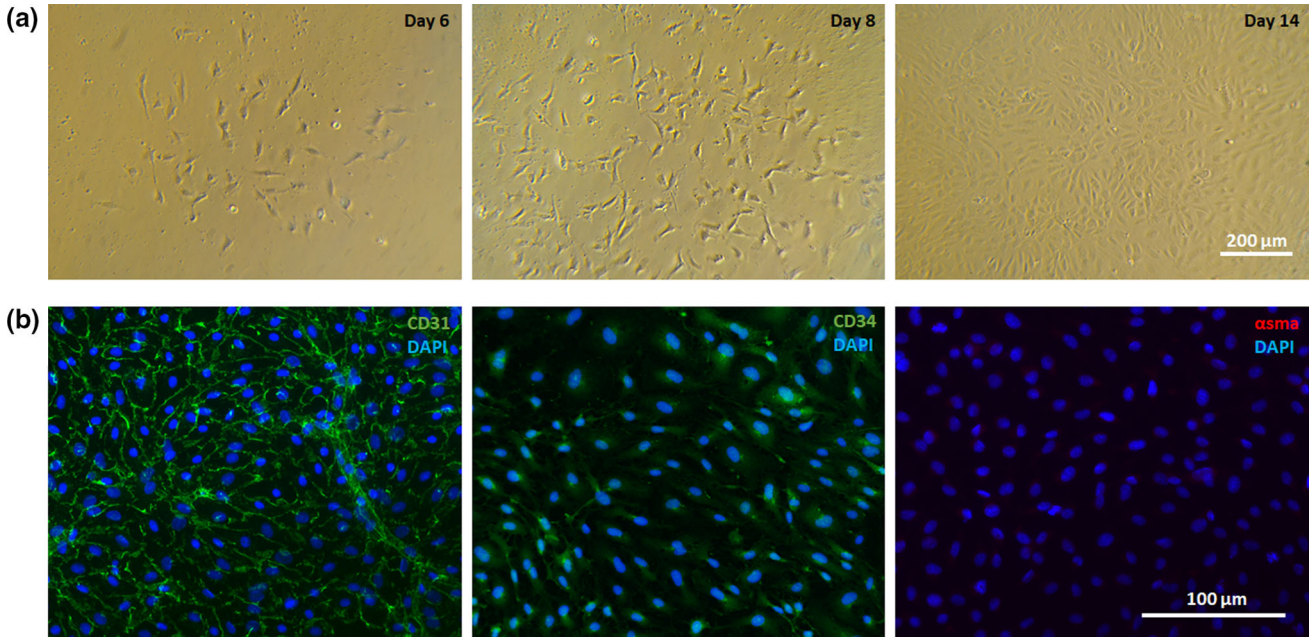

FIGURE 1. (a) Brightfield images of EPC colony progression over time showing spindle-shaped cells at early stages and adopting a cobblestone morphology. (scale bar of 200 μm applies to all subset images); (b) Immunostaining of EPCs at passage 2 for positive EPC markers (CD31, CD34) and negative EPC marker (αSMA). (n = 3, scale bar of 100 μm applies to all subset images).

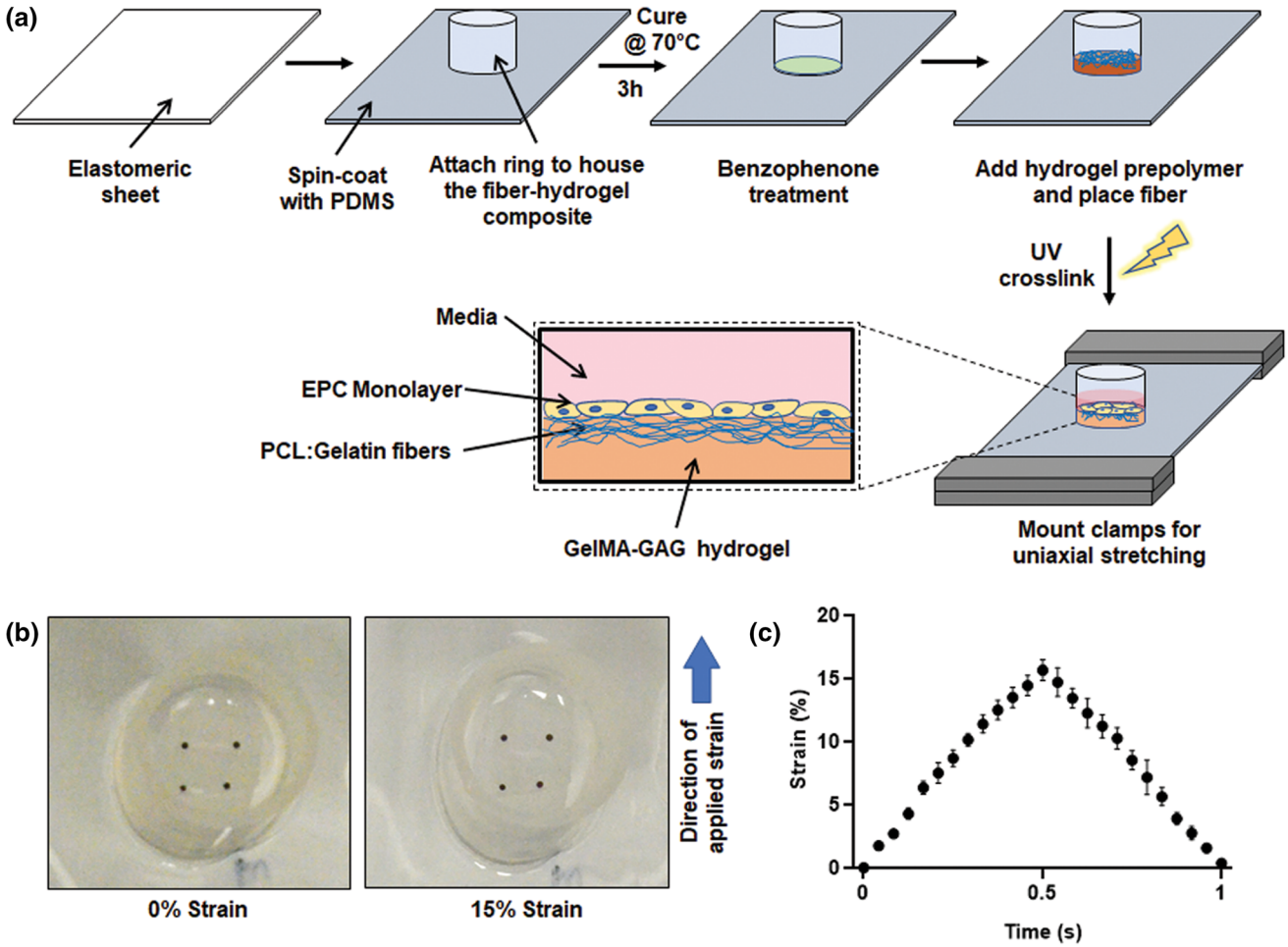

FIGURE 2. (a) Schematic summarizing the attachment of fiber-reinforced hydrogel composite onto benzophenone treated elastomeric membranes. (b) Fiducial markers placed on the composites used for tracking strains. (c) Validation of cyclic strain on fiber-reinforced hydrogel composite as a function of time (n = 4).

structure formation. All these results taken together show that our isolated cells were EPCs.

Fabrication and Validation of Uniaxial Mechanical Strain on Valve-Mimetic Composites

The valve-mimetic composites were designed based on our previous publication.[31] The diseased valve-mimetic composites used in this study were characterized as reported in our previous work conducted on healthy valve-mimetic composites[31] for porosity, pore size, enzymatic degradation, swelling ratio, and gelatin and GAG elution (Supplementary Figs. 1, 2, and 3). The detailed results are provided in the supplemental section. Additionally, both our healthy and diseased composites exhibited mechanical properties that were comparable to the native porcine aortic valve, but the diseased composites were able to reach higher radial strains compared to the healthy composites (Supplemental Fig. S4). Following their characterization, these valve-mimetic composites were attached to an elastomeric PDMS membrane to validate the strain transmission on our uniaxial stretcher.

The schematic depicting the attachment of the composite onto the elastomeric membrane is provided in Fig. 2(a). We first validated that the valve-mimetic composites were completely attached to the elastomeric membrane through the benzophenone treatment and confirm that the uniaxial cyclic stretching was able to transfer the strains through the composites. To test this, we marked the fiber composites with fiducial markers and performed the cyclic stimulation. MATLAB-based image analysis by tracking fiducial markers (Fig. 2b) revealed that the composites were able to experience 15% strains provided by the stretching of the membrane (Fig. 2c). This also shows that treating benzophenone on to the elastomeric membrane aided in the attachment of the valve-mimetic composites onto our stretching platform.

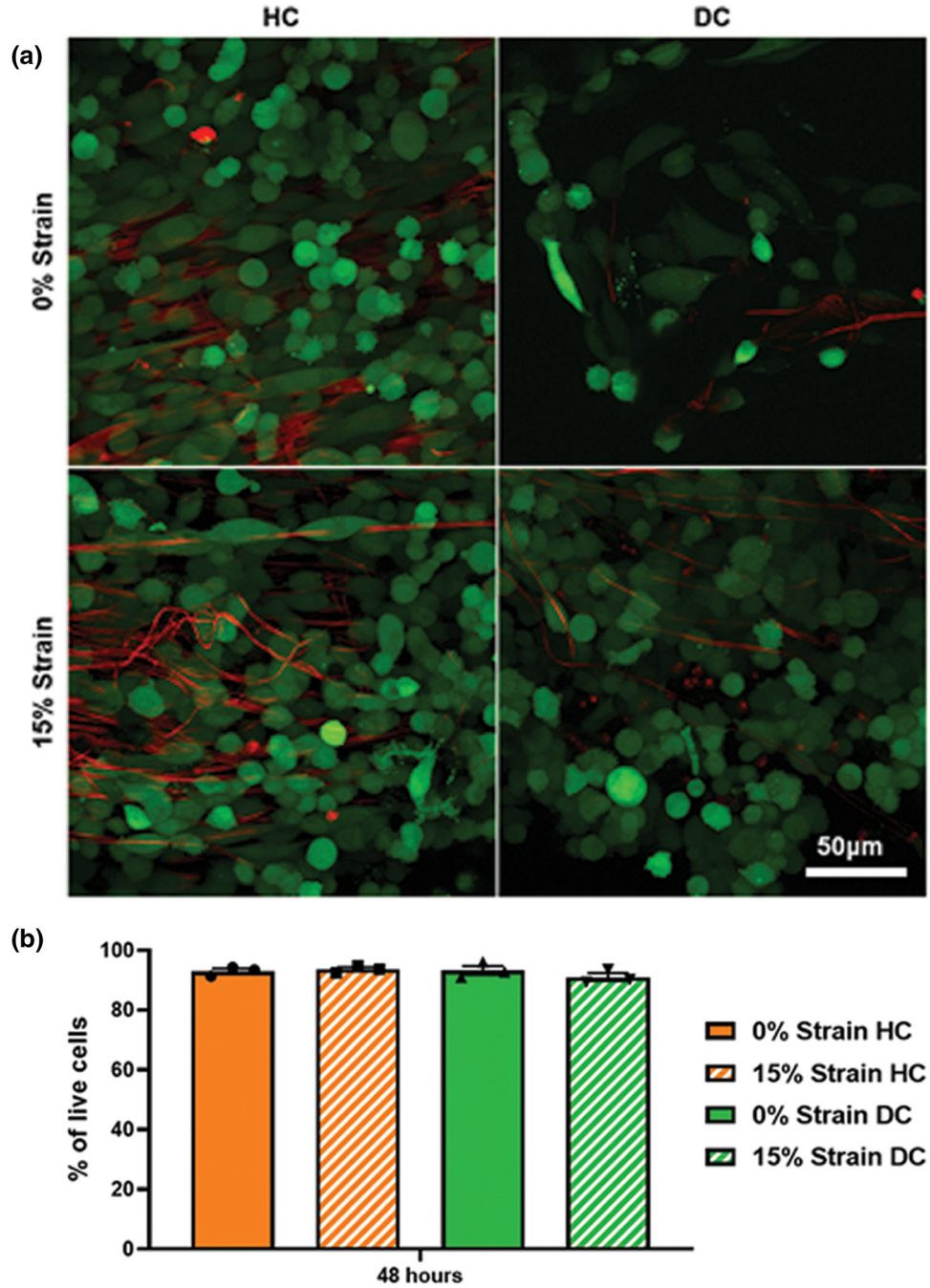

FIGURE 3. (a) Live/Dead staining of EPCs cultured on healthy (HC) and diseased (DC) composites at 0% and 15% strains. (b) Percentage of live cells quantified in all tested conditions by counting the total number of live and dead cells. (n = 3, scale bar of 50 μm applies to all images in the figure).

Cell Viability Was Maintained in Both Healthy and Diseased Composites

We investigated the viability of EPCs on our valve-mimetic composites to ensure that the engineering and attachment of the composites did not affect the cells. Live/dead staining revealed that the cells were able to attach to the composite surface and showed more cells on healthy composites compared to diseased composites in the static condition (Fig. 3a, Supplemental Fig. S5). Unstrained diseased composites had significantly lower total cell numbers compared to all other conditions ($p < 0.05$) (Supplemental Fig. S5). Quantification of the live/dead staining showed that EPCs expressed more than 90% viability at the end of

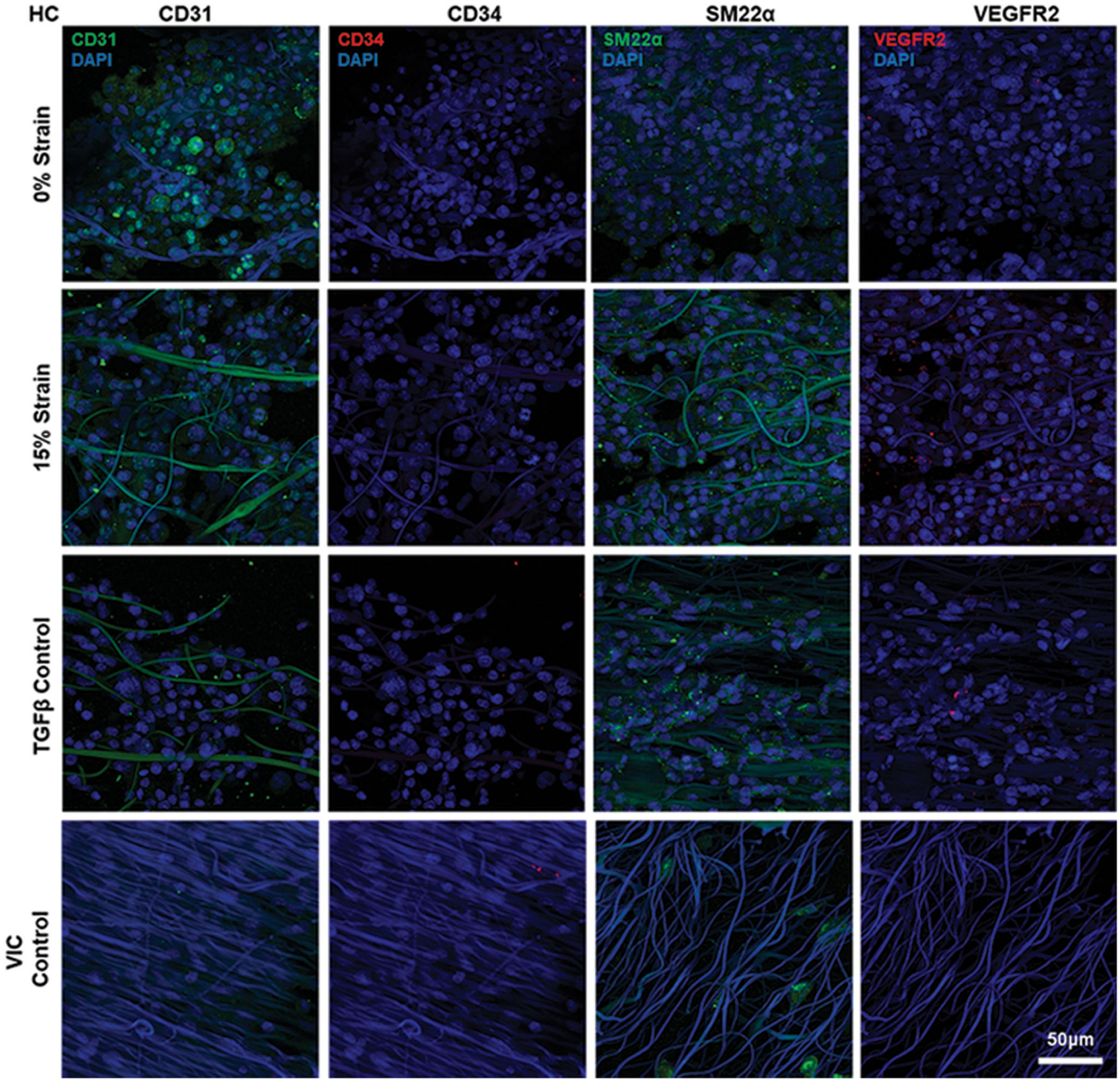

FIGURE 4. Immunostaining of EPCs cultured on healthy composites (HC) under the different treatment conditions stained for CD31, CD34, SM22α, and VEGFR2 at the end of 48 hours. VICs were seeded on the surface of the composites to serve as controls and DAPI was used to stain the nuclei. (n = 3, scale bar of 50 μm applies to all immunostained images in the figure).

48 hours on all conditions (Fig. 3b), confirming that the engineering and attachment of the composite constructs did not cause any adverse effects on the cells. The percentage of live cells did not show any statistical significance between the different tested conditions (Fig. 3b). Analysis of raw dead cell numbers indicated significantly increased dead cells in strained diseased composites compared to unstrained diseased composites (p = 0.008) (Supplemental Fig. S5).

Cyclic Strain Resulted in Altered Phenotype of EPCs

We asked if the EPCs were able to undergo phenotypic change when subjected to static or strained conditions with the TGFβ treatment serving as positive controls. We also wanted to evaluate the role of healthy and diseased GAG compositions on EPCs. Figure 4 depicts the various treatment conditions of the healthy composite. Qualitatively, we observe that the 15% strained EPC conditions showed a reduced expression in the endothelial marker, CD31, compared

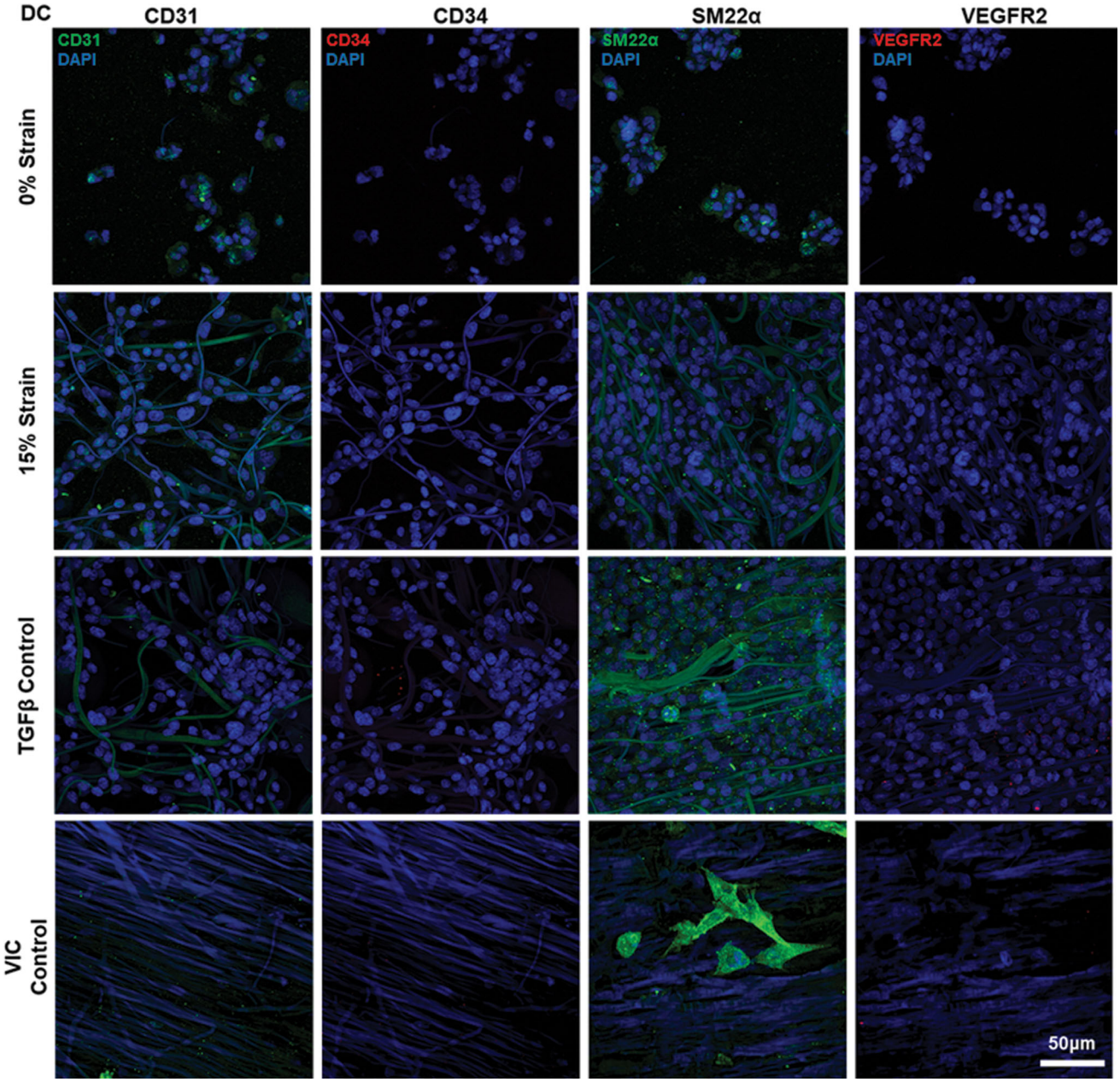

FIGURE 5. Immunostaining of EPCs cultured on diseased composites (DC) under the different treatment conditions stained for CD31, CD34, SM22α, and VEGFR2 at the end of 48 hours. VICs were seeded on the surface of the composites to serve as controls and DAPI was used to stain the nuclei. (n = 3, scale bar of 50 μm applies to all immunostained images in the figure).

with the static conditions. Interestingly, we were able to observe that the smooth muscle cell marker, SM22α, showed more expression in EPCs subjected to 15% strain compared to its static counterpart. Virtually, no expression for the hematopoietic stem cell marker, CD34, and vascular endothelial marker, VEGFR2, was observed in EPCs cultured under the static and strained conditions. We know that the TGFβ treatment causes the EPCs to undergo mesenchymal transition; similarly, our healthy composites treated with TGFβ showed relatively no expression of endothelial, hematopoietic, and vascular markers but did express the smooth muscle cell marker. To further confirm our observations, we seeded VICs on the surface of these healthy composites and stained them for the same set of markers. As shown in Fig. 4 VIC control, the cells did not express any CD31, CD34, and VEGFR2; however, samples did show positive expression for the smooth muscle cell marker.

As stated, we performed staining with the same set of markers for EPCs cultured on the diseased composites (Fig. 5). Similar to the healthy composites, the overall

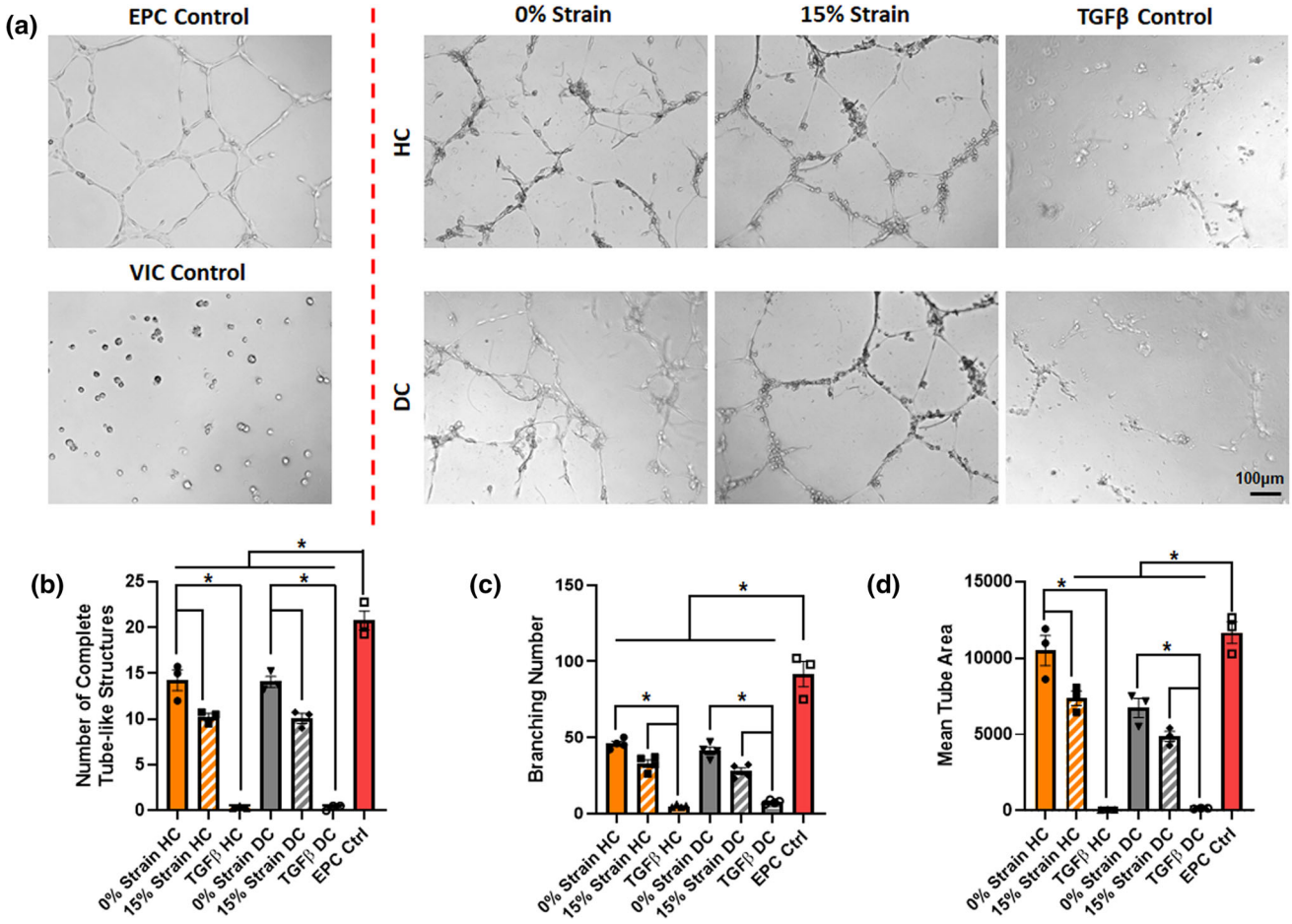

FIGURE 6. (a) Matrigel tube-formation assay-EPC control showing defined tube structures with VIC control not forming any networks. 0% strain conditions expressed comparable tube structures to 15% strain conditions but TGFβ controls revealed reduced tube formations. (b) Quantification of number of vascular tube structures per image field. (c) Quantification of number of branching points and (d) mean tube area. (n = 4, * represents p < 0.05, scale bar of 100 μm applies to all images in the figure). HC and DC represent healthy and diseased valve-mimetic composites respectively.

marker expression pattern remained the same for CD34 and VEGF2. However, the static conditions had comparatively lesser number of cells on the composite compared to the strained samples. This aligns with our live/dead staining (Fig. 3a, Supplemental Fig. S5) where the number of cells in the static diseased composites were lower compared to the strained condition. The VIC control samples also revealed the same pattern with the cells not expressing any CD31, CD34, and VEGFR2; but the VICs on these diseased composites showed much greater expression for the smooth muscle cell marker.

EPCs Expressed Higher SM22α Gene in Mechanically Strained Healthy Composites

To further validate the phenotypic shifts observed in the strained samples as compared to the static counterparts we performed quantitative RT-PCR and assessed expression. We observed that healthy composites under static conditions had undetectable levels of the SM22α gene while there was a 6-fold increase in the 15% strained counterparts as compared to the 15% strained diseased composites (Supplemental Fig. 6). In fact, diseased composites showed a more than 3-fold increase in SM22α gene expression compared to their healthy counterparts except for the 15% strained samples (Supplemental Fig. 6). Individually, the diseased composite and 15% strained healthy composites promoted mesenchymal phenotype in EPCs. However, this increase in SM22α gene expression was inhibited when 15% strain was applied to diseased composites. This data suggested that the application of cyclic stretch may be able to promote a mesenchymal phenotype in EPCs.

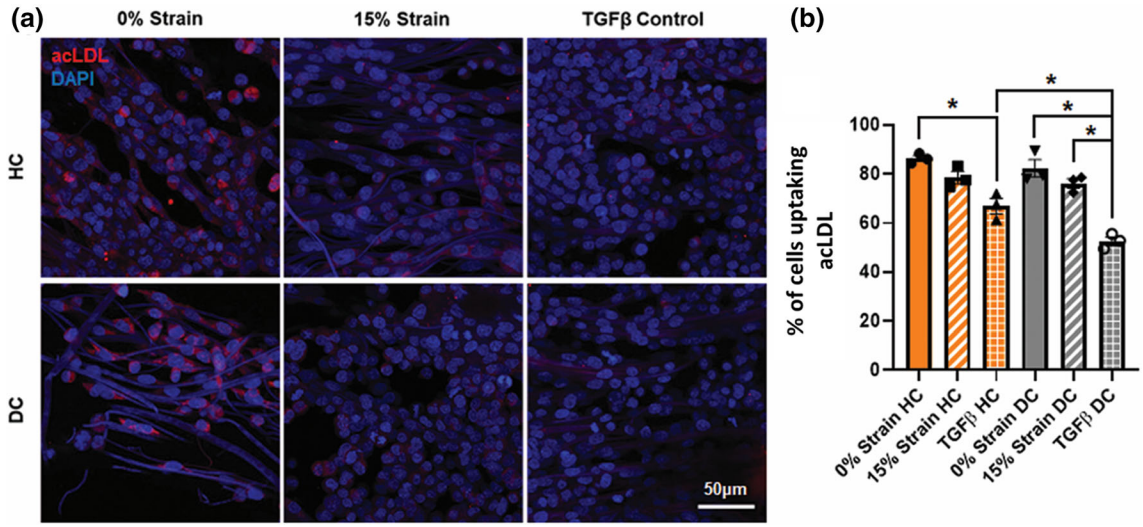

FIGURE 7. (a) acLDL uptake assay- EPCs cultured on 0% strain conditions were able uptake more acLDL compared to 15% strain conditions with TGFβ treated samples showed the least uptake. (b) Quantification of percentage of cells expressing acLDL uptake also showed the reduced trend of acLDL uptake with cyclically strained conditions ($n = 4$, * represents $p < 0.05$, scale bar of 50 μm applies to all images in the figure). HC and DC represent healthy and diseased valve-mimetic composites respectively.

EPCs Demonstrate Lesser Vasculogenic Potential after Mechanical Strain

At the end of 48 hours, the composites were trypsinized to dissociate the EPCs, and the cells were reseeded onto Matrigel-coated plates. Figure 6(a) revealed that 0% and 15% strain conditions had comparable vascular tube structure formation but were less defined than the EPC controls. This could be due to the cells losing their vasculogenic ability when cultured on the composites. The static conditions showed more vascular tube networks compared to 15% strain conditions. The TGFβ treated controls had reduced tubular network formations compared to the 0 and 15% strained conditions and reveals that this treatment causes the EPCs to lose their vasculogenic potential and express a more mesenchymal-like behavior. The negative control VICs did not form any networks owing to not possessing any vasculogenic activity. Quantification of the number of vascular tubes per image field (Fig. 6b) indicated that both the 15% strain conditions of healthy ($p = 0.013$) and diseased ($p = 0.01$) composites had significantly reduced vascular tube networks compared to their respective static healthy and diseased counterparts. Additionally, TGFβ controls expressed the least vascular tubes in healthy ($p < 0.0001$) and diseased ($p < 0.0001$) composites compared to 15% strained healthy and diseased composites respectively. All of the 0% and 15% conditions, and TGFβ controls were significantly lower ($p < 0.0001$) compared to EPCs controls that involved direct seeding of EPCs from a culture flask to Matrigel coated plates.

Further quantification of branching points (Fig. 6c) revealed that both the 15% strain conditions of healthy ($p = 0.09$) and diseased ($p = 0.07$) composites expressed a reduced trend in the number of branches compared to their respective static healthy and diseased counterparts. Additionally, a similar observation was noted in the mean tube area quantification with 15% strain conditions of healthy composites ($p = 0.036$) had reduced mean tube compared to static healthy composites. However, the 15% strained diseased composites ($p = 0.3$) showed only a reduced trend in the mean tube area compared to their static counterparts. Interestingly, the EPC controls ($p = 0.8$) showed similar mean tube area compared to the static healthy composites. Overall, our results show that the EPCs in strained conditions were losing its vasculogenic properties shown by a reduced trend in number of complete tubes, tube branching, and mean tube area.

Mechanical Strain Reduced Endothelial Function in EPCs

At the end of 48 hours, the composites were treated with acLDL for 4 hours before being fixed and stained using DAPI. The acLDL uptake assay measures the functionality of the EPCs. From Fig 7a, we observed that the cells in the static conditions had a higher uptake of acLDL compared to the 15% strain and TGFβ treated conditions. Further quantification (Fig. 7b) revealed that the 15% strain in healthy composites ($p = 0.29$) had a lower percentage of EPCs that were able

to uptake acLDL compared to the static conditions, but no statistical significance was observed. We observed that the TGFβ controls showed a similar trend of reduced uptake compared to the 15% strain healthy composites ($p = 0.054$) and were significantly lower compared to the EPCs cultured on healthy composites at static conditions ($p = 0.0014$). Our diseased composites also expressed a similar finding with the EPCs showing reduced trend of acLDL uptake in the 15% strain conditions compared to static conditions ($p = 0.34$). Additionally, TGFβ controls expressed a significantly lower percentage of cells uptaking acLDL compared to the 15% strain ($p = 0.0002$) and static conditions ($p < 0.0001$). Overall, these results showed that 15% strained EPCs are losing their endothelial function, observed by the reduced acLDL uptake in the cells.

DISCUSSION

Since the discovery of EPCs, studies have focused on understanding their differentiation in response to shear stress.[25,34,26,6,1] It has been established that EPCs from the bone marrow are released to the injury sites and differentiate to mature endothelial cells *via* increased expression of endothelial cell markers and cell adhesion molecules.[25,15,26,6,1] However, it is evident that adhesive EPCs may also be subjected to cyclic strains along with shear stresses within vasculature.[32] Additionally, heart valve leaflets experience cyclic strains and shear stresses which is dependent on the location on the leaflet.[35] While previously EPCs have been shown to be a potential source of both endothelial and interstitial cells for heart valve tissue engineering,[38] it is important to understand EPC behavior under mechanical forces subjected on heart valve. This study focused on understanding the effect of valve-mimetic cyclic mechanical conditioning on EPC differentiation by culturing EPCs on valve-mimetic fiber-reinforced hydrogel composites.

By culturing cord blood-derived EPCs on our previously reported valve-mimetic composites,[31] we were able to show that cells were able to attach and maintain viability. We noticed that EPCs attached in lower numbers on the diseased composites compared to healthy composites (Fig 3a); however, at the end of cyclic mechanical stimulation for 48 hours, the cells showed an increase in their numbers. A similar result showing an increase in cell number was reported in a recent study where EPCs cultured in 2D cultures under cyclic strain to evaluate the survival, proliferation, and maintenance of EPC cultures.[9] We did not notice any significant difference in percentage live cells between the healthy and diseased composites in their strained conditions.

Phenotypic changes were observed in the static and strained conditions by immunostaining (Figs. 4 and 5). These results showed decreased expression in the endothelial marker in the strained samples compared to the static conditions and a similar trend was observed in both the healthy and diseased composites. Additionally, no expression of hematopoietic stem cell marker (CD34) was observed in both our healthy and diseased composites regardless of their mechanical stimulation. These immunostaining results with loss of hematopoietic marker, reduced endothelial expression and the positive expression of SM22α lead us to believe that the EPCs' angiogenic and arteriogenic properties are reduced. Additionally, matrigel tube formation assay results (Fig. 6) also agreed with the immunostaining results where the strained conditions revealed less defined tubular structure formations, reduced tube branching, and mean tube area compared to its static counterparts. The strained conditions had longer tubular structures compared to the static conditions (Fig. 6a). A reason for this behavior might be dictated by the mechanical stiffness of the composite. It has been shown that increasing stiffness from 1 kPa to 20 kPa can cause the EPCs to become more mesenchymal-like with increased expression of alpha smooth muscle actin and longer vessel formation in the Matrigel assay.[21] These results combined with the increased transgelin (SM22α) expression suggest that the EPCs were undergoing a phenotypic change. Sales *et al.* were the first to show that ovine EPCs can differentiate into valve-like cells in the presence of TGFβ with an increased expression in smooth muscle cell markers.[37] Their findings were in alignment with our TGFβ controls where the cells did not express any of the commonly observed EPC markers such as CD31, CD34, and VEGFR2, but showed positive expression for transgelin (SM22α), a smooth muscle cell marker. However, the study involving dynamic rotational culture of EPCs had incorporated TGFβ, an endothelial-mesenchymal transition mediator to induce the differentiation process in 5 days of culture.[37] Given this previous observation, we expect to observe an increased expression of the smooth muscle cell markers over longer periods of time. Additionally, these TGFβ controls reduced vascular tube network formation in both our healthy and diseased composites when EPCs were cultured on Matrigel which could be attributed to the loss of vasculogenic property and increased mesenchymal-like phenotype.

Apart from the Matrigel assay, we also measured the acLDL uptake to test the functionality of EPCs cultured on valve-mimetic composites. Our results (Fig. 7) revealed that the percentage of EPCs express-

ing acLDL was reduced in our healthy and diseased composites cultured at 15% strain compared to static conditions. Our functional assays revealed that the cells cultured at 15% strain conditions expressed reduced vasculogenic potential and lower percentage of cells expressing acLDL. which could denote that the EPCs were losing their characteristic vascular and endothelial function with increasing mesenchymal-like cell behavior.

Previously it was observed that shear stresses promoted vasculogenic properties of circulating EPCs by promoting an endothelial phenotype.[13] Our study showed that cyclic strain reduced vasculogenic properties of EPCs by promoting a mesenchymal cell type. With insights from our study, it can be speculated that a careful control of shear stresses and cyclic strains may be helpful in obtaining endothelial and mesenchymal cell types from EPCs. This is specifically relevant when considering EPCs as an autologous cell source for heart valve applications as the heart valve leaflets experience both cyclic strains and shear stresses.[35]

Another noteworthy observation was that diseased scaffolds did not produce significant differences in responses as compared to healthy composite scaffolds. It has been previously observed that in EPC laden scaffolds with or without TGFβ, sulfated GAG production did not increase even after 15 days.[37] In another instance, it was observed that GAG mimetic [OTR_{4131}] which is a sulfated dextran mimetic, increased proliferation of EPCs; however, these experiments were carried out for at least 5 days.[31] Given our diseased scaffolds were marked by a 4-fold increase in GAGs, primarily hyaluronic acid and chondroitin sulfate, it is possible that EPC function and phenotype may not be highly sensitive to these GAGs especially in an acute time frame of 2 days. We also observed a pattern where the cells on the static diseased conditions were lower, but the mechanical stimulation of the diseased conditions resulted in similar cell proliferation compared to the strained healthy conditions. This observation suggests that the cyclic mechanical strain predominates EPC proliferation over biochemical cues in the time periods studied here. Longer time periods would aid in understanding these differences more in depth. Future studies will include studying the same set of markers for longer periods with samples stimulated on a biaxial stretcher as this mode of stimulation better mimics the strains experienced in the native valve. Longer time points and additional stretch conditions might also reveal any differential effects the EPCs might express due to the varied GAG compositions. We will also study the expression of extracellular markers such as Collagen I, Collagen III, and fibronectin to understand the ability of EPCs to regenerate tissue. Further experiments tailored to understand the underlying signaling pathways that result in EPC differentiation will also be evaluated.

CONCLUSION

In conclusion, we show that the valve-mimetic anisotropic fiber-reinforced hydrogel composites were able to provide an ideal environment for the EPCs to maintain high cell viability. Our immunostaining results revealed that the mechanically-strained EPCs were able to express smooth muscle cell marker with reduced expression of endothelial, vascular, and hematopoietic markers which could be due to the cells undergoing differentiation. Our functional assays also showed a similar trend with strained EPCs forming less vascular tube networks and reduced expression of acLDL. Overall, our study serves as initial evidence that valve-mimetic cyclic mechanical stimulation can initiate the differentiation of EPCs into both endothelial and smooth muscle-like cells.

SUPPLEMENTARY INFORMATION

The online version contains supplementary material available at https://doi.org/10.1007/s13239-022-00623-5.

ACKNOWLEDGMENTS

We acknowledge funding support from the National Science Foundation under grant number CMMI-1452943, and Arkansas Biosciences Institute.

CONFLICT OF INTEREST

All authors declare they have no conflicts of interest.

REFERENCES

[1]Angelos, M. G., M. A. Brown, L. L. Satterwhite, V. W. Levering, N. T. Shaked, and G. A. Truskey. Dynamic adhesion of umbilical cord blood endothelial progenitor cells under laminar shear stress. *Biophys. J.* 99(11):3545–3554, 2010. https://doi.org/10.1016/j.bpj.2010.10.004.

[2]Asahara, T., T. Murohara, A. Sullivan, M. Silver, R. van der Zee, T. Li, et al. Isolation of putative progenitor endothelial cells for angiogenesis. *Science*. 275(5302):964–967, 1997. https://doi.org/10.1126/science.275.5302.964.

[3]Balachandran, K., P. W. Alford, J. Wylie-Sears, J. A. Goss, A. Grosberg, J. Bischoff, et al. Cyclic strain induces dual-mode endothelial-mesenchymal transformation of the cardiac valve. *Proc Natl Acad Sci USA*. 108(50):19943–19948, 2011. https://doi.org/10.1073/pnas.1106954108.

[4]Bono, N., D. Pezzoli, L. Levesque, C. Loy, G. Candiani, G. B. Fiore, et al. Unraveling the role of mechanical stimulation on smooth muscle cells: a comparative study between 2D and 3D models. *Biotechnol. Bioeng*. 113(10):2254–2263, 2016.

[5]Ceccarelli, J., A. Cheng, and A. J. Putnam. Mechanical strain controls endothelial patterning during angiogenic sprouting. *Cell. Mol. Bioeng*. 5(4):463–473, 2012. https://doi.org/10.1007/s12195-012-0242-y.

[6]Cheng, B. B., Z. Q. Yan, Q. P. Yao, B. R. Shen, J. Y. Wang, L. Z. Gao, et al. Association of SIRT1 expression with shear stress induced endothelial progenitor cell differentiation. *J. Cell. Biochem*. 113(12):3663–3671, 2012. https://doi.org/10.1002/jcb.24239.

[7]Dainese, L., A. Guarino, B. Micheli, V. Biagioli, G. Polvani, F. Maccari, et al. Aortic valve leaflet glycosaminoglycans composition and modification in severe chronic valve regurgitation. *J. Heart Valve Dis*. 22(4):484–490, 2013.

[8]Diez, M., M. M. Musri, E. Ferrer, J. A. Barbera, and V. I. Peinado. Endothelial progenitor cells undergo an endothelial-to-mesenchymal transition-like process mediated by TGFbetaRI. *Cardiovasc. Res*. 88(3):502–511, 2010.

[9]Doyoung, K., and Y. Son. Mechanical cyclic stretch regulate angiogenic abilities of endothelial progenitor cells. *Cytotherapy*. 22(5):S191–S192, 2020.

[10]Egusa, H., M. Kobayashi, T. Matsumoto, J. Sasaki, S. Uraguchi, and H. Yatani. Application of cyclic strain for accelerated skeletal myogenic differentiation of mouse bone marrow-derived mesenchymal stromal cells with cell alignment. *Tissue Eng. Part A*. 19(5–6):770–782, 2013. https://doi.org/10.1089/ten.TEA.2012.0164.

[11]Gao, D., D. Nolan, K. McDonnell, L. Vahdat, R. Benezra, N. Altorki, et al. Bone marrow-derived endothelial progenitor cells contribute to the angiogenic switch in tumor growth and metastatic progression. *Biochim. Biophys. Aacta*. 1796(1):33–40, 2009. https://doi.org/10.1016/j.bbcan.2009.05.001.

[12]George, A. L., P. Bangalore-Prakash, S. Rajoria, R. Suriano, A. Shanmugam, A. Mittelman, et al. Endothelial progenitor cell biology in disease and tissue regeneration. *J. Hematol. Oncol*. 4:24, 2011.

[13]Ghaleh, A. S., S. Saghati, R. Rahbarghazi, A. Hassani, L. S. Kaleybar, M. H. Geranmayeh, et al. Static and dynamic culture of human endothelial cells encapsulated inside alginate-gelatin microspheres. *Microvasc. Res*.137:104174, 2021. https://doi.org/10.1016/j.mvr.2021.104174.

[14]Hess, D. C., C. A. Sila, A. J. Furlan, L. R. Wechsler, J. A. Switzer, and R. W. Mays. A double-blind placebo-controlled clinical evaluation of MultiStem for the treatment of ischemic stroke. *Int. J. Stroke*. 9(3):381–386, 2014. https://doi.org/10.1111/ijs.12065.

[15]Hess, D. C., L. R. Wechsler, W. M. Clark, S. I. Savitz, G. A. Ford, D. Chiu, et al. Safety and efficacy of multipotent adult progenitor cells in acute ischaemic stroke (MASTERS): a randomised, double-blind, placebo-controlled, phase 2 trial. *Lancet Neurol*. 16(5):360–368, 2017. https://doi.org/10.1016/S1474-4422(17)30046-7.

[16]Huang, A. H., Y.-U. Lee, E. A. Calle, M. Boyle, B. C. Starcher, J. D. Humphrey, et al. Design and use of a novel bioreactor for regeneration of biaxially stretched tissue-engineered vessels. *Tissue Eng. Part C*. 21(8):841–851, 2015.

[17]Khang, A., P. Ravishankar, A. Krishnaswamy, P. K. Anderson, S. G. Cone, Z. Liu, et al. Engineering anisotropic biphasic Janus-type polymer nanofiber scaffold networks via centrifugal jet spinning. *J. Biomed. Mater. Res. Part B*. 105(8):2455–2464, 2017. https://doi.org/10.1002/jbm.b.33791.

[18]Ladhoff, J., B. Fleischer, Y. Hara, H. D. Volk, and M. Seifert. Immune privilege of endothelial cells differentiated from endothelial progenitor cells. *Cardiovasc. Res*. 88(1):121–129, 2010. https://doi.org/10.1093/cvr/cvq109.

[19]Lei, Y., and Z. Ferdous. Design considerations and challenges for mechanical stretch bioreactors in tissue engineering. *Biotechnol. Progr*. 32(3):543–553, 2016. https://doi.org/10.1002/btpr.2256.

[20]Li, Y., G. Huang, M. Li, L. Wang, E. L. Elson, T. J. Lu, et al. An approach to quantifying 3D responses of cells to extreme strain. *Sci. Rep*. 6:19550, 2016. https://doi.org/10.1038/srep19550.

[21]Link, P. A., D. Farkas, L. Farkas, and R. L. Heise. Pulmonary endothelial progenitor cells demonstrate phenotypic shift from altered substrate mechanics. *Am. J. Resp. Crit. Care*. 195:4309, 2017.

[22]Matsumoto, T., Y. C. Yung, C. Fischbach, H. J. Kong, R. Nakaoka, and D. J. Mooney. Mechanical strain regulates endothelial cell patterning in vitro. *Tissue Eng*. 13(1):207–217, 2007. https://doi.org/10.1089/ten.2006.0058.

[23]Moonen, J.-R.A.J., G. Krenning, M. G. L. Brinker, J. A. Koerts, M. J. A. van Luyn, and M. C. Harmsen. Endothelial progenitor cells give rise to pro-angiogenic smooth muscle-like progeny. *Cardiovasc Res*. 86(3):506–515, 2010.

[24]Nova-Lamperti, E., F. Zúñiga, V. Ormazábal, C. Escudero, and C. Aguayo. Vascular regeneration by endothelial progenitor cells in health and diseases. *Microcirc. Rev*. 2016. https://doi.org/10.5772/64529.

[25]Obi, S., H. Masuda, T. Shizuno, A. Sato, K. Yamamoto, J. Ando, et al. Fluid shear stress induces differentiation of circulating phenotype endothelial progenitor cells. *Am. J. Physiol. Cell Physiol*. 303(6):C595-606, 2012. https://doi.org/10.1152/ajpcell.00133.2012.

[26]Obi, S., K. Yamamoto, and J. Ando. Effects of shear stress on endothelial progenitor cells. *J. Biomed. Nanotechnol*. 10(10):2586–2597, 2014. https://doi.org/10.1166/jbn.2014.2014.

[27]Von Offenberg, Sweeney N., P. M. Cummins, E. J. Cotter, P. A. Fitzpatrick, Y. A. Birney, E. M. Redmond, et al. Cyclic strain-mediated regulation of vascular endothelial cell migration and tube formation. *Biochem. Biophys. Res. Commun*. 329(2):573–582, 2005. https://doi.org/10.1016/j.bbrc.2005.02.013.

[28]Patel, J., P. Donovan, and K. Khosrotehrani. Concise review: functional definition of endothelial progenitor cells: a molecular perspective. *Stem Cells Transl. Med*. 5(10):1302–1306, 2016.

[29]Porras, A. M., J. A. Westlund, A. D. Evans, and K. S. Masters. Creation of disease-inspired biomaterial environments to mimic pathological events in early calcific aortic valve disease. *Proc. Natl. Acad. Sci. USA*. 115(3):E363–E371, 2018. https://doi.org/10.1073/pnas.1704637115.

[30]Ravishankar, P., A. Khang, M. Laredo, and K. Balachandran. Using dimensionless numbers to predict centrifugal jet-spun nanofiber morphology. *J. Nanomater*. 2019:2019, 2019.

[31]Ravishankar, P., A. Ozkizilcik, A. Husain, and K. Balachandran. Anisotropic fiber-reinforced glycosaminoglycan hydrogels for heart valve tissue engineering. *Tissue Eng Part A*. 2020. https://doi.org/10.1089/ten.TEA.2020.0118.

[32]Ravishankar, P., M. A. Zeballos, and K. Balachandran. Isolation of endothelial progenitor cells from human umbilical cord blood. *J. Visual. Exp*. 2017. https://doi.org/10.3791/56021.

[33]Ribatti, D. The discovery of endothelial progenitor cells. An historical review. *Leuk Res*. 31(4):439–444, 2007.

[34]Rössig, L., C. Urbich, T. Brühl, E. Dernbach, C. Heeschen, E. Chavakis, et al. Histone deacetylase activity is essential for the expression of HoxA9 and for endothelial commitment of progenitor cells. *J. Exp. Med*. 201(11):1825–1835, 2005.

[35]Saberianpour, S., M. Heidarzadeh, M. H. Geranmayeh, H. Hosseinkhani, R. Rahbarghazi, and M. Nouri. Tissue engineering strategies for the induction of angiogenesis using biomaterials. *J. Biol. Eng*. 12(1):1–15, 2018.

[36]Sacks, M. S., W. David Merryman, and D. E. Schmidt. On the biomechanics of heart valve function. *J. Biomech*. 42(12):1804–1824, 2009. https://doi.org/10.1016/j.jbiomech.2009.05.015.

[37]Sales, V. L., G. C. Engelmayr Jr., B. A. Mettler, J. A. Johnson Jr., M. S. Sacks, and J. E. Mayer Jr. Transforming growth factor-beta1 modulates extracellular matrix production, proliferation, and apoptosis of endothelial progenitor cells in tissue-engineering scaffolds. *Circulation*. 114(1 Suppl):I193–I199, 2006.

[38]Sales, V. L., B. A. Mettler, G. C. Engelmayr Jr., E. Aikawa, J. Bischoff, D. P. Martin, et al. Endothelial progenitor cells as a sole source for ex vivo seeding of tissue-engineered heart valves. *Tissue Eng. Part A*. 16(1):257–267, 2010.

[39]Urbich, C., and S. Dimmeler. Endothelial progenitor cells: characterization and role in vascular biology. *Circ. Res*. 95(4):343–353, 2004.

[40]Vaughan, E. E., and T. O'Brien. Isolation of circulating angiogenic cells. *Methods Mol. Biol*. 916:351–356, 2012. https://doi.org/10.1007/978-1-61779-980-8_25.

[41]Xue, Y., P. Ravishankar, M. A. Zeballos, V. Sant, K. Balachandran, and S. Sant. Valve leaflet-inspired elastomeric scaffolds with tunable and anisotropic mechanical properties. *Polym. Adv. Technol*. 31(1):94–106, 2020.

[42]Yuk, H., T. Zhang, G. A. Parada, X. Liu, and X. Zhao. Skin-inspired hydrogel–elastomer hybrids with robust interfaces and functional microstructures. *Nat. Commun*. 7(1):1–11, 2016.